SUPPORTING INFORMATION for

Probing the impact of local structural dynamics of conformational epitopes on antibody recognition

Yu Liang[1], Miklos Guttman[1], Tad M. Davenport[1,2], Shiu-Lok Hu[3], Kelly K. Lee[1,]*

[1] Department of Medicinal Chemistry, University of Washington, Seattle WA, 98195
[2] Current address: Laboratory of Molecular and Cellular Imaging, National Heart, Lung, and Blood Institute, Bethesda, MD 20814
[3] Department of Pharmaceutics, University of Washington, Seattle WA, 98195

The supporting information includes data for protein purification and the complete hydrogen/deuterium-exchange mass spectrometry data in the form of butterfly plots and deuterium up-take plots for each observable peptide. A peptic digest sequence coverage map is also included. Lastly, Octet biolayer interferometry sensorgrams are provided.

Supporting information contents:

Figure S1. SDS-PAGE, native PAGE and gel filtration analysis of purified FL, ΔV3, ΔV1/V2 and $Core_e$. (A) SDS-PAGE analysis of purified gp120s. (B) Blue native-PAGE analysis of purified gp120s. (C) Gel filtration analysis of purified gp120s. (D) Sequence alignment for FL, ΔV3, ΔV1/V2 and $Core_e$.

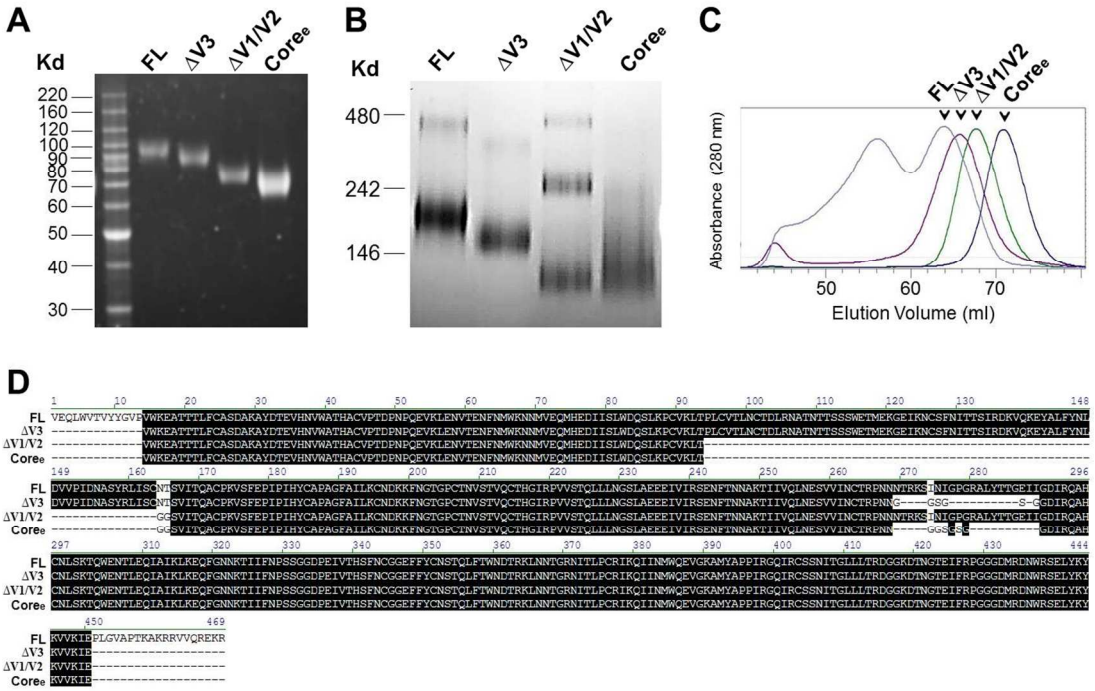

Figure S2. Observable peptides coverage map of unliganded full-length YU2 gp120. The primary gp120 sequence is underlined according to the observable peptide fragments used for H/D exchange measurements. The inner domain residues are shown in pink. The outer domain residues are shown in grey. The bridging sheets residues are shown in red. V1-V5 loops and the CD4 binding loop are highlighted as yellow.

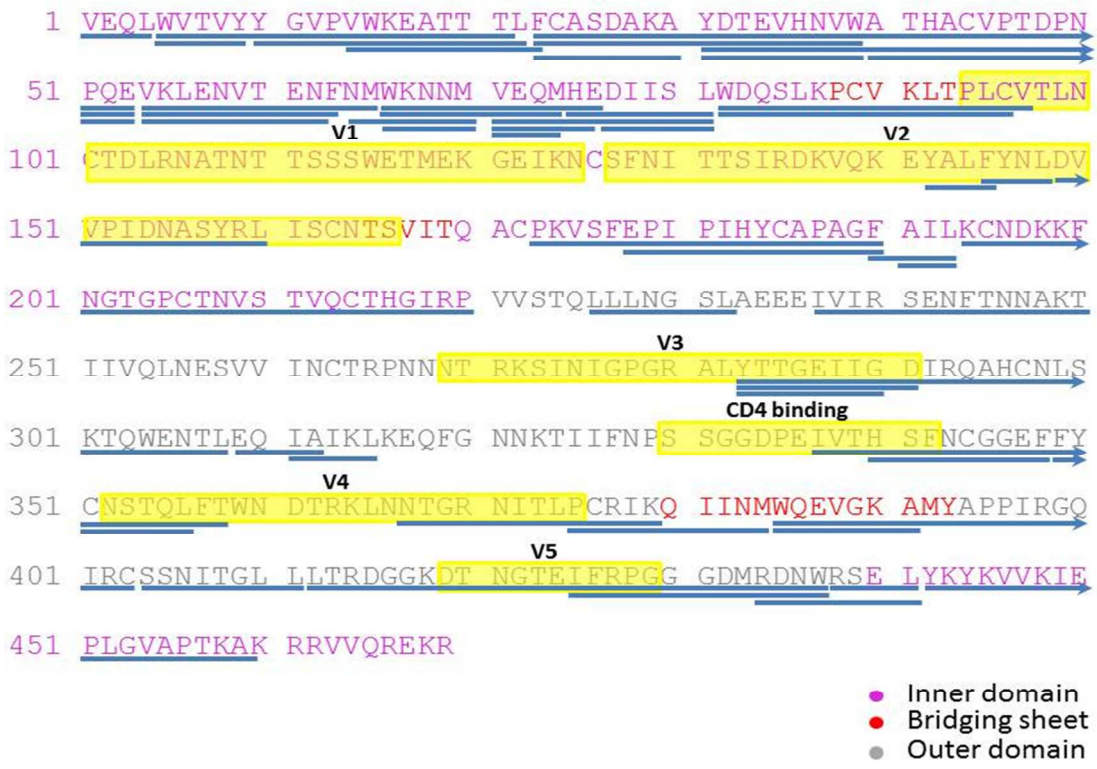

Figure S3. Structural dynamics in gp120 monomers deleted with variable loops detected by H/D exchange shown in butterfly plots. (A) Butterfly plots for FL (top) and FL+sCD4 (bottom). (B) Butterfly plots for FL (top) and ΔV3 gp120 (bottom). (C) Butterfly plots for FL (top) and ΔV1/V2 gp120 (bottom). (D) Butterfly plots for FL (top) and $Core_e$ gp120 (bottom). The exchange is shown by each peptide at the midpoint in primary sequence. The variable loops are highlighted in grey. Under each butterfly plot there is a difference plot showing the difference in percent exchange at each point. The positions of differences are colored in grey ovals.

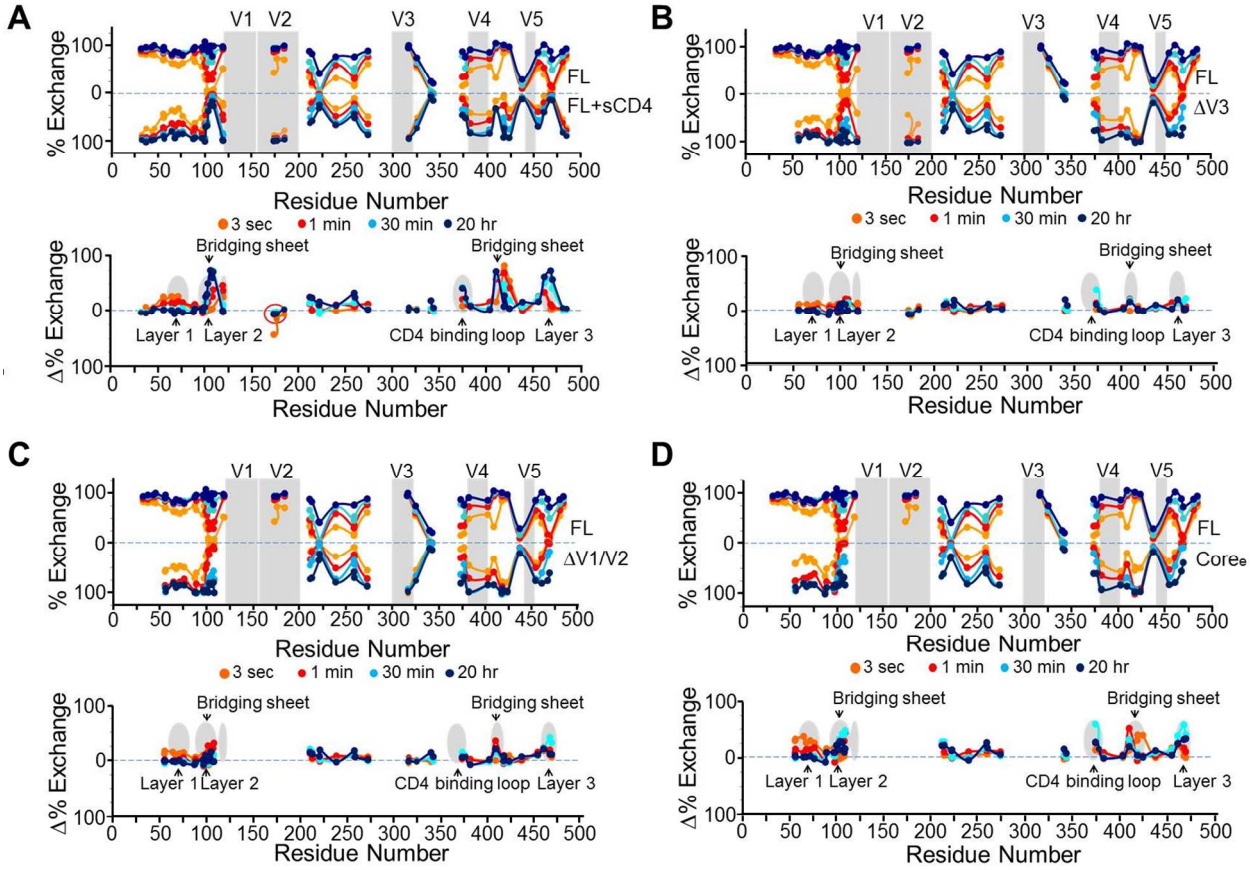

Figure S4. Structural dynamics in gp120 monomers deleted with variable loops compared to FL+sCD4 as detected by H/D exchange. (A) Butterfly plots for ΔV3 (top) and FL+sCD4 (bottom). (B) Butterfly plots for ΔV1/V2 (top) and FL+sCD4 (bottom). (C) Butterfly plots for $Core_e$ (top) and FL+sCD4 (bottom). Explains for the plots were shown in Fig. S3. (D) Differences in deuterium exchange for ΔV3 and FL+sCD4, ΔV1/V2 and FL+sCD4, $Core_e$ and FL+sCD4, plotted on the heat map (from left to right). Differences in deuterium exchange at 3 sec were shown in the upper row. Differences in deuterium exchange at 30 min were shown in the bottom row. The degrees of change between the two proteins are colored from white (<20% difference) to orange (20%-50% difference) to red (>50% difference).

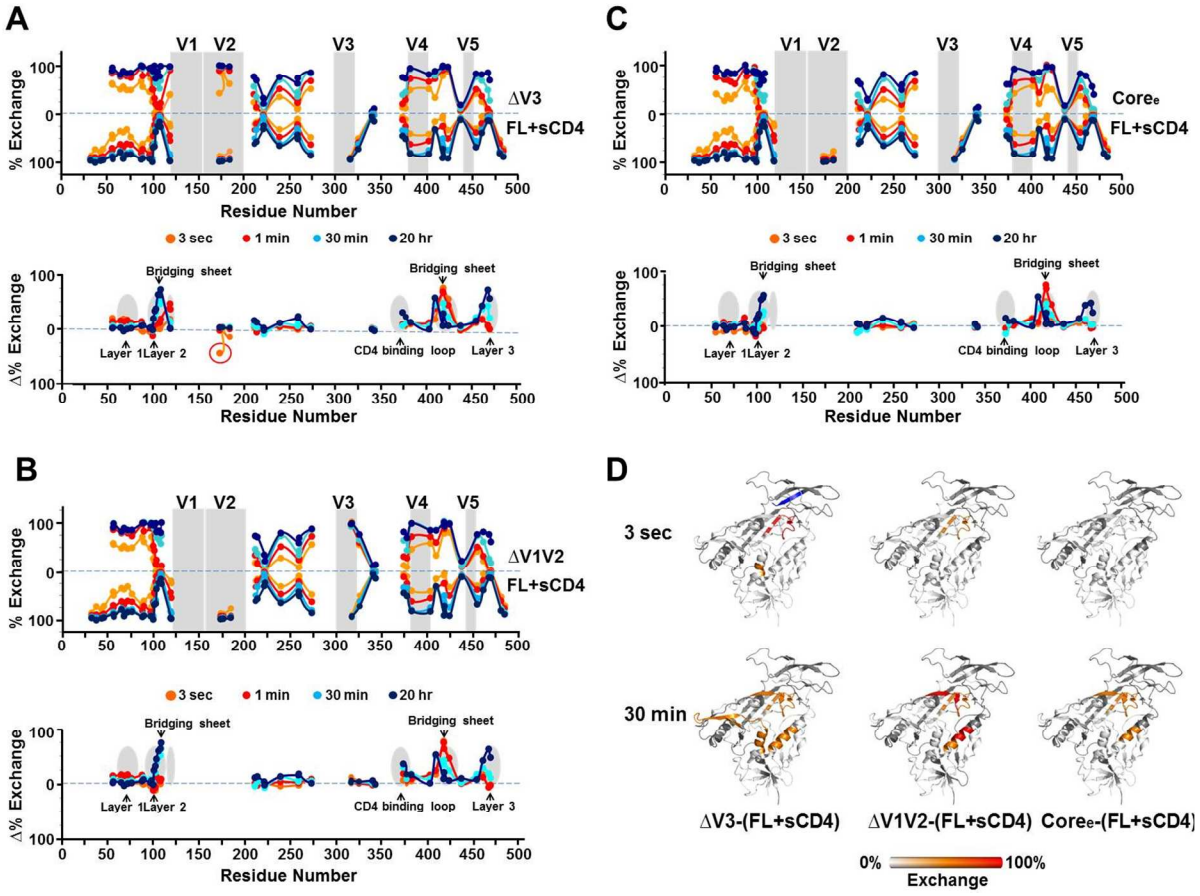

Figure S5. Deuterium exchange profiles for the various observable peptides of gp120s. Deuterium exchange (%) is shown for monomeric FL (blue), ΔV3 (purple), ΔV1/V2 (green), $Core_e$ (red) and FL+sCD4 (yellow) as a function of time (in seconds). Error bars represent standard deviations from different observed peptide charge states and duplicate experiments.

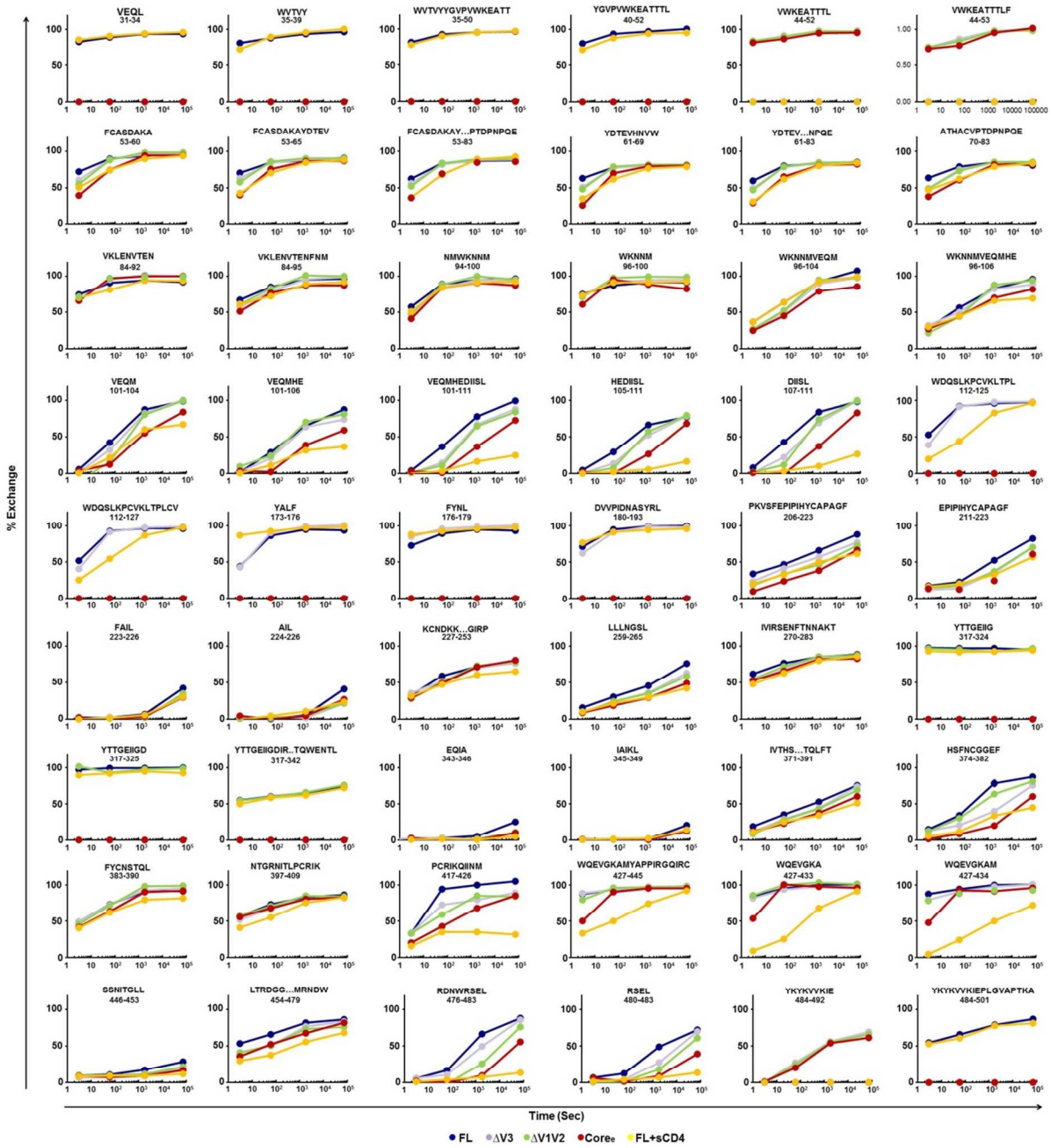

Figure S6. Comparisons of H/D exchange profiles of ΔV3, ΔV1/V2 and $Core_e$. (A) Butterfly plots for ΔV3 (top) and $Core_e$ (bottom). (B) Butterfly plots for ΔV1/V2 (top) and $Core_e$ (bottom). (C) Butterfly plots for ΔV3 (top) and ΔV1/V2 (bottom). Explanations for the butterfly plots were referred to Fig. 2.

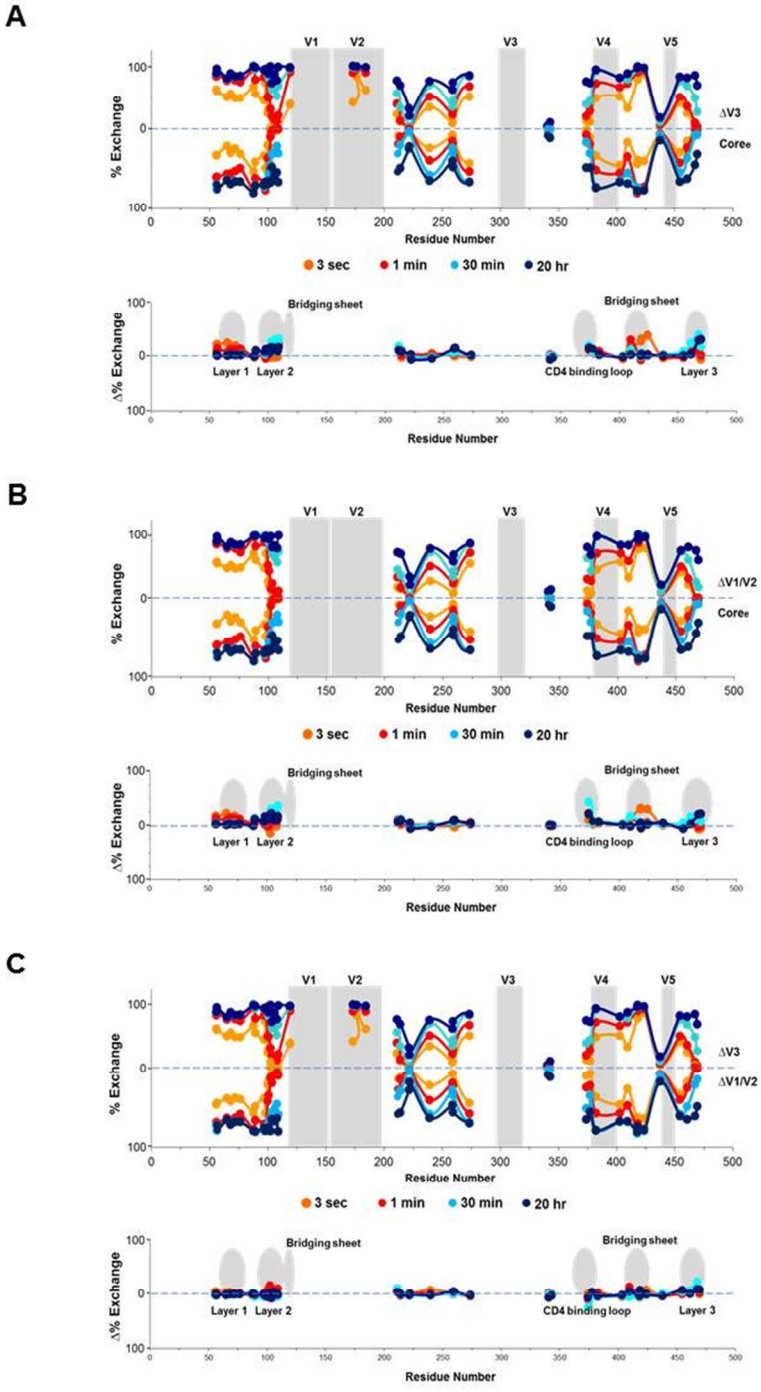

Figure S7. Octet biolayer interferometry binding curves for CD4i binding antibodies. Binding curves for FL, ΔV3, ΔV1/V2 and $Core_e$ in serial concentrations (indicated under each graph) binding to 17b, 48d, A32 and N5i5 captured by AHC biosensors are shown. The binding model curves (best-fit 1:1) are colored in red. The four gp120s, FL, ΔV3, ΔV1/V2 and $Core_e$ are shown in different columns (from left to right). The four antibodies, 17, 48d, A32 and N5i5 are shown in different rows (from top to bottom). X-axis is time and Y-axis is binding response (in nanometers).

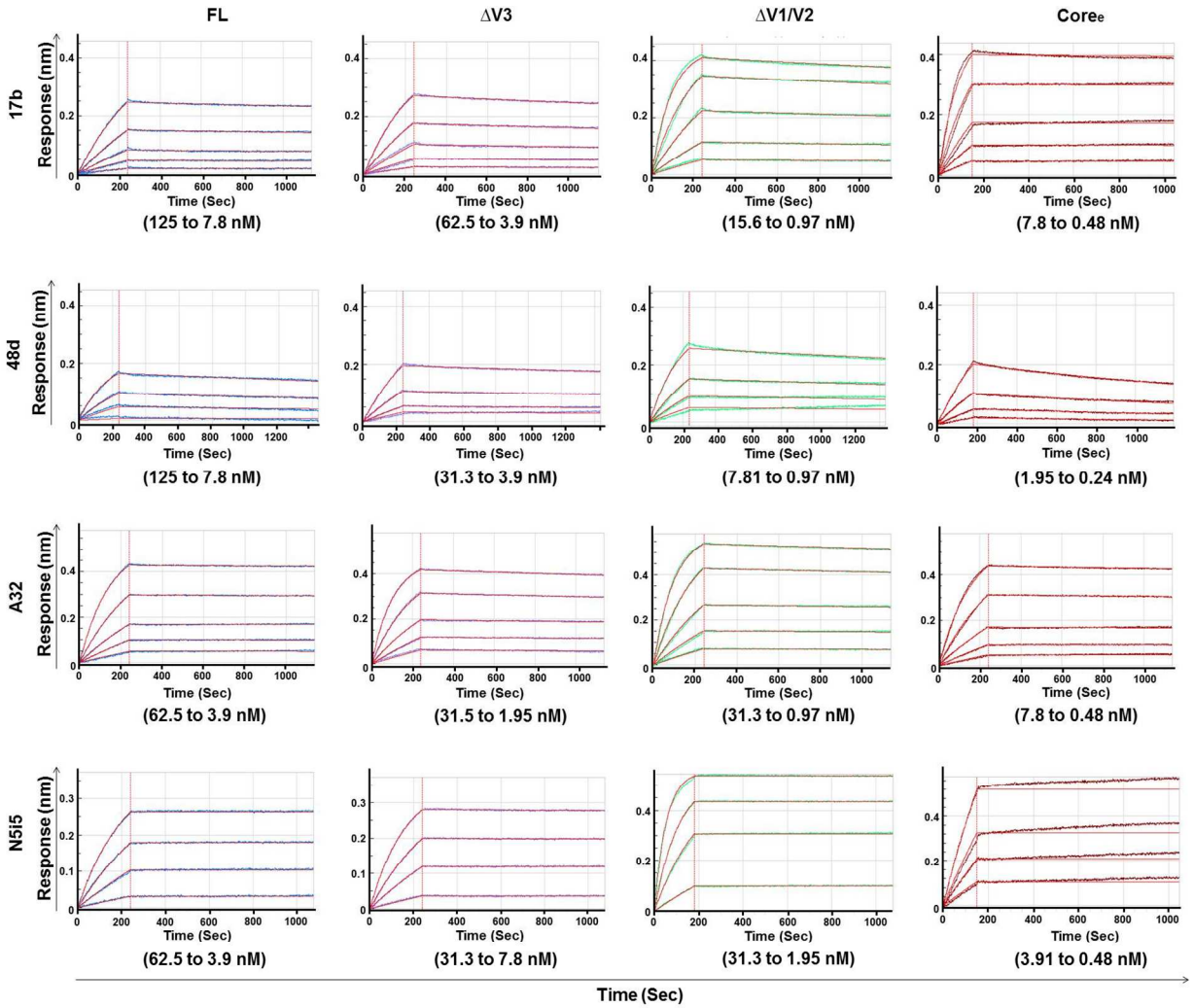

Figure S8. Octet biolayer interferometry binding curves for CD4-IgG2 and CD4BS binding antibodies. Binding curves for FL, ΔV3, ΔV1/V2 and $Core_e$ in serial concentrations (indicated under each graph) binding to CD4-IgG2, NIH45-46, VRC01, VRC03, F105 and b12 captured by AHC biosensors are shown. The binding model curves (best-fit 1:1) are colored in red. The four gp120s, FL, ΔV3, ΔV1/V2 and $Core_e$ are shown in different columns (from left to right). The CD4-IgG2, NIH45-46, VRC01, VRC03, F105 and b12 are shown in different rows (from top to bottom). X-axis is time and Y-axis is binding response (in nanometers).

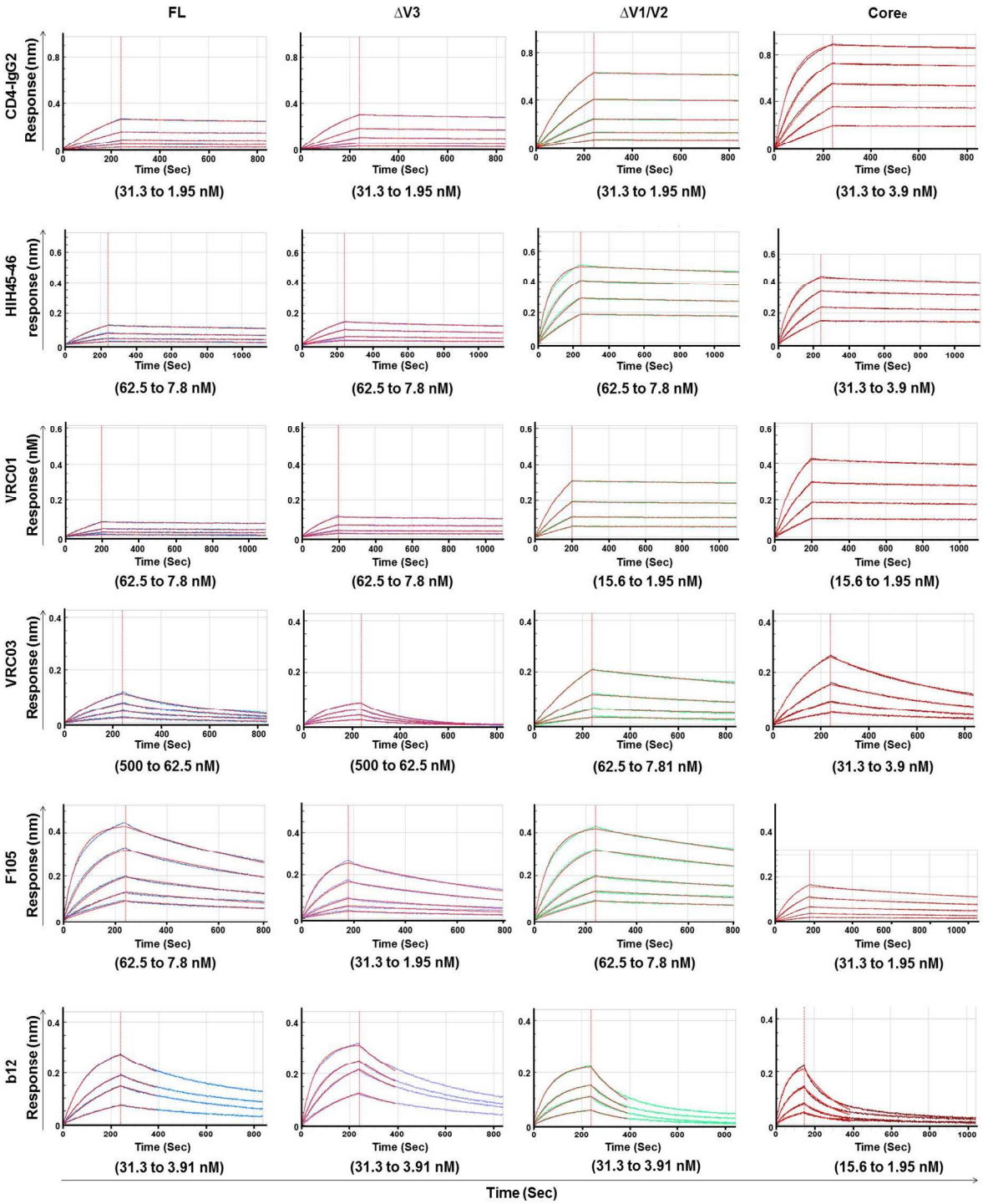
FL
ΔV3
ΔV1/V2
Core e
CD4-IgG2
Response (nm)
(31.3 to 1.95 nM)
(31.3 to 1.95 nM)
(31.3 to 1.95 nM)
(31.3 to 3.9 nM)
HIH45-46
response (nm)
(62.5 to 7.8 nM)
(62.5 to 7.8 nM)
(62.5 to 7.8 nM)
(31.3 to 3.9 nM)
VRC01
Response (nM)
(62.5 to 7.8 nM)
(62.5 to 7.8 nM)
(15.6 to 1.95 nM)
(15.6 to 1.95 nM)
VRC03
Response (nm)
(500 to 62.5 nM)
(500 to 62.5 nM)
(62.5 to 7.81 nM)
(31.3 to 3.9 nM)
F105
Response (nm)
(62.5 to 7.8 nM)
(31.3 to 1.95 nM)
(62.5 to 7.8 nM)
(31.3 to 1.95 nM)
b12
Response (nm)
(31.3 to 3.91 nM)
(31.3 to 3.91 nM)
(31.3 to 3.91 nM)
(15.6 to 1.95 nM)
Time (Sec)